13

Characterization of Activated Carbons Produced from Oleaster Stones

Hale Sütcü
Zonguldak Karaelmas University
Turkey

1. Introduction

Activated carbon has a porous structure surrounded by carbon atoms and therefore is a material with adsorbent capability. The most important parameter that is put into consideration to investigate its chemical characterization is porosity. Pore size determines how adsorption takes place in pores (Marsh & Reinoso, 2006). In accordance with IUPAC, pores are classified into three different sizes. Pores less than 2,0 nm are classified as micropores, those in the range of 2,0-50 nm mesopores and those greater than 50 nm macropores (IUPAC).

The selection of raw material for the production of activated carbon is made on the basis of carbon amount, mineral matter and sulfur content, availability, cost, and shelf life (Kroschwitz,1992). Raw material may be of vegetable, animal and mineral origin and the production can be carried out by means of physical and chemical activation depending on the type of raw material.

The physical activation method generally involves carbonization and activation stages (Singh, 2001). In the activation stage oxidizing agents are used such as carbondioxide and steam and thus form pores and canals (Jankowska et al., 1991).

Chemical activation involves a carbonization stage where a chemical activating agent that is in the form of a solution or dry is blended with the raw material. Chemicals employed in chemical activation (potassium hydroxide, phosphoric acid, zinc chloride etc.) are effective at decomposing the structure of the raw material and forming micropores (Marsh & Reinoso, 2006).

The literature has many articles dealing with activated carbons produced from raw material using both the chemical and physical activation methods. Materials frequently used as raw material of vegetable origin include corncobs (Sun et al., 2007; Aworn et al., 2009; Preethi et al., 2006), hazelnuts (Demiral et al., 2008; Soleimani & Kaghazchi, 2007), olives (Yavuz et al., 2010), nuts (Yeganeh et al., 2006; Aygun et al., 2003), peaches (Kim, 2004), loquat stones (Sütcü & Demiral, 2009), wood (Ould-Idriss et al., 2011; Sun & Jiang, 2010) and bamboo (Ip et al., 2008), those of animal origin bones (Moreno-Pirajan et al., 2010) and hide waste (Demiral & Demiral, 2008), and those of mineral origin coal (Alcaniz-Monge et al., 2010; Cuhadaroglu & Uygun, 2008; Liu et al., 2007; Sütcü & Dural, 2007), petroleum coke (Lu et al., 2010) and rubber (Gupta et al., 2011; Nabais et al., 2010).

In this study I produced activated carbons from chars obtained through the carbonization of oleaster stones by physical, chemical and chemical+physical activation, and performed their surface characterization.

2. Experimental

2.1 Material and its structural characterization

The oleasters used in this study were obtained from a green grocer and their stones removed. The stones were washed clean and dried at 105°C for 24 hours.

The structural analysis of the oleaster stones were carried out by proximate and ultimate analyses, thermogravimetric analysis (TG), fourier transform infrared spectroscopy (FTIR) and scanning electron microscopy (SEM). The results regarding the proximate and ultimate analyses are given in Table 1.

The TG analysis was performed using a PL 1500TGA apparatus from ambient to 800°C at a heating rate of 10 °C/min and a nitrogen flow rate of 100 ml/min.

The FTIR spectrum was taken by means of a Perkin Elmer Spectrum One apparatus at wavelengths ranging from 4000 to 650 cm^{-1}.

The SEM image was obtained using a JEOL JSM model 5410 LV scanning electron microscope.

Ash[a]	Volatile Matter [a]	Fixed Carbon [a]	C [b]	H [b]	N [b]	S [b]
0.57	74.27	25.16	48.16	0.66	3.44	0.29

Table 1. The results of proximate and ultimate analyses of oleaster stones (a. on dry basis, %, b. on dry and ash free basis, %)

2.2 Production of chars and their structural characterization

The stones were subjected to carbonization at a heating rate of 10 °C/min, a carbonization temperature of 600 °C and a nitrogen flow rate of 100 ml/min, and held at that temperature for 1 h. The carbonization was performed in a tube furnace of internal diameter 6 cm and length 110 cm. The chars were reduced to a size range of 0.5-1.0 mm to make them ready for the production of activated carbon.

The structural analysis of the chars were conducted by proximate and ultimate analyses, TG analysis, FTIR spectroscopy and SEM. Table 2 gives the results from the proximate and ultimate analyses undertaken.

The FTIR spectrum was taken using a Perkin Elmer Spectrum One apparatus within a wavelength range of 4000-650 cm^{-1}.

The SEM image was obtained using a JEOL JSM model 5410 LV scanning electron microscope .

Ash[a]	Volatile Matter [a]	Fixed Carbon [a]	C [b]	H [b]	N [b]
2.30	10.40	87.30	62.60	2.45	0.63

Table 2. Results from analyses of chars (a. on dry basis, %, b. on dry and ash free basis, %)

2.3 Activated carbon production

2.3.1 Physical Activation (PH)

The production of activated carbon from chars by physical activation was conducted in a tube furnace at carbonization temperatures of 650°C, 750°C and 850°C. The chars were heated up to the above-mentioned temperatures at a nitrogen atmosphere in a flow rate of 100 ml/min and a heating rate of 10 °C/min, and subjected to a CO_2 atmosphere with a flow

rate of 100 ml/min. The chars thus obtained were kept in an desiccator. The chars produced by means of this method were designated as PH650, PH750 and PH850, respectively.

2.3.2 Chemical Activation (CH)

The production of chemical activation from chars was carried out using the chemical KOH at carbonization temperatures of 650ºC, 750ºC and 850ºC. The mixture prepared in such a way that the char/KOH ratio would be 1/1 (mass ratio) was mixed with water of 10ml and held in a drying oven at 50 ºC for 24 hours. The mixture was then heated up to the aforementioned temperatures at a heating rate of 10 ºC/min and a nitrogen flow rate of 100 ml/min, and kept at that temperature for 1 hour. The activated carbons produced were boiled with 0.5 N HCI for 30 minutes and washed with distilled water until their pH was 6.5. Finally, they were dried in a vacuum drying oven and kept in an desiccator. The activated carbons thus obtained were designated as CH650, CH750 and CH850, respectively.

2.3.3 Sequential Activation (Chemical+Physical, CHPH)

The chars were blended with 10ml of distilled water in such a way that the char/KOH ratio would be 1/1 (mass ratio) and held in a drying oven for 24 hours. After that, this mixture was heated up to 650 ºC, 750 ºC and 850 ºC at a nitrogen flow rate of 100 ml/min and a heating rate of 10 ºC/min and was held at these temperatures under CO_2 with a flow rate of 100 ml/min. After the activated carbons produced were boiled with 0,5 N HCI for 30 minutes, they were washed with distilled water until a pH value of 6.5 was achieved, dried in a vacuum drying oven at 105 ºC for 24 hours and kept in an desiccator. The activated obtained through this method are denoted by CHPH650, CHPH750 and CHPH850, respectively.

2.4 Strucural characterization of activated carbons

Structural characterization of the activated carbons was carried out by FTIR spectroscopy, SEM and a Quantachrome Autosorb Automated Gas Sorption System.

The FTIR spectra of the activated carbons were taken by means of a Perkin Elmer Spectrum One apparatus at wavelengths in the range of 4000 to 650 cm^{-1}.

The SEM images were obtained using a JEOL JSM model 5410 LV scanning electron microscope.

The iodine number of the activated carbons was determined in accordance with ASTM D 4607-94.

Surface analyses were performed by nitrogen adsorption at -196ºC using a Quantachrome Autosorb Automated Gas Sorption System. Prior to adsorption, the activated carbons were outgassed under vacuum conditions at 250ºC for 3 hours. Adsorption isotherms were obtained at pressures in the range of 10^{-5}-1.0. The surface areas and pore volumes were determined by means of Brunauer-Emmett-Teller (BET) and t-pilot software and pore size distribution using density functional theory (DFT) software.

3. Results and discussion

3.1 Structural analysis of oleaster stones and chars

Figure 1 gives the results from TG analysis carried out on oleaster stones. The decomposition of oleaster stones takes place in three stages. The first stage, which occurs at temperatures ranging from 30 ºC to 140 ºC involves moisture loss (Popescu et al., 20111). The other stages are

related to the release of volatiles resulting from the decomposition of hemicellulose, cellulose and lignin (Tongpoothorn et al., 2011; Luangkiattikhun et al., 2008; Antal, 1982). In the second stage occuring at 140 ºC-245 ºC, hemicellulose decomposes as well as cellulose which also starts to disintegrate. Within this temperature range, the maximum decomposition temperature and rate were established to be 222 ºC and 1,50%, respectively. The last stage, which takes place within a temperature range of 245 ºC and 600 ºC, is characterized by the decomposition of cellulose and lignin. The maximum decomposition temperature in this stage was found to be 333 ºC and the maximum decomposition rate 6.71%.
The amount of char remaining as a result of TG analysis of oleaster stones in nitrogen atmosphere is 25.57%.

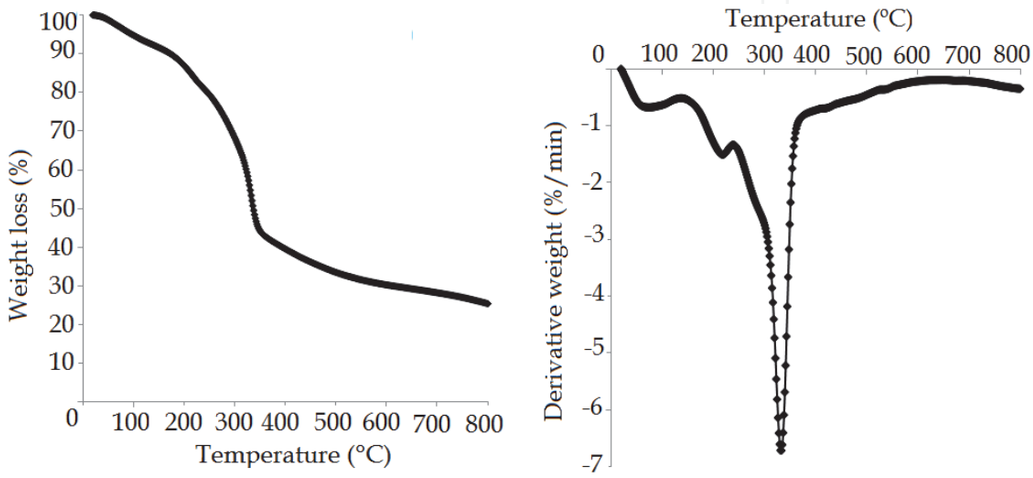

Fig. 1. Graph depicting the results from thermogravimetric and differential thermogravimetric analyses of oleaster stones.

Figure 2 gives the FTIR spectra of oleaster stones and chars obtained from them. An interpretation of the FTIR spectra reveals the existence of functional groups occurring in the structure.
The band observed at 3600-3200 cm^{-1} is indicative of the –OH stretching peak and existence of phenol, alcohol and carboxylic containing hydroxyl groups. This band, which is present in oleaster stones, do not exist in chars. This can be attributed to the decomposition of the structure and removal of the groups containing hydroxyl groups.
The band at 3000-2800 cm^{-1} indicates the presence of an aliphatic –CH stretching. This band is visible in oleaster stones but not in chars.
The band at around 1700 cm^{-1} denotes the existence of carbonyl/carboxyl groups and can be observed in oleaster stones.
The 1600-1500 cm^{-1} band, which is visible in both oleaster stones and chars, indicates the presence of an aromatic C=C ring stretching.
The bands at 1450-1300 cm^{-1} denotes the existence of C-H vibrating alkene groups. This band which exist in oleaster stones occurs in chars more densely.
The bands observed at 1240-1000 cm^{-1} indicates the existence of phenolic and alcoholic groups, and were identified in the FTIR spectra of oleaster stones and chars. The bands at 900-600 cm^{-1} denotes the presence of aromatic ring structures and are visible in both oleaster stones and chars.

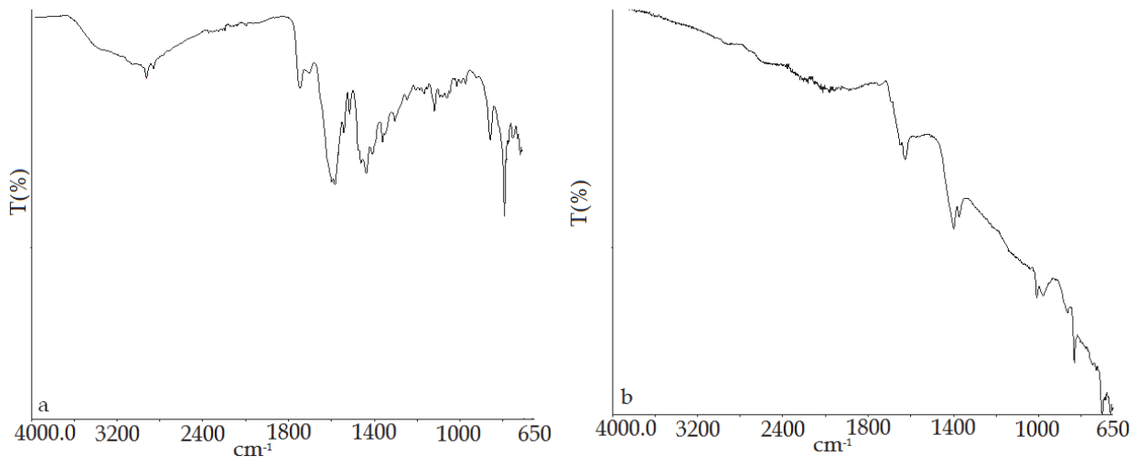

Fig. 2. FTIR spectra of (a) oleaster stones and (b) chars produced from them

Figure 3 gives SEM micrographs of oleaster stones and chars obtained from them.
It is clear from the SEM micrograph of oleaster stones that they have a fibrous structure. Chars produced at a carbonization temperature of 600ºC were also determined to have a fibrous structure, a heterogeneous size and pores without any homogeneous distribution.

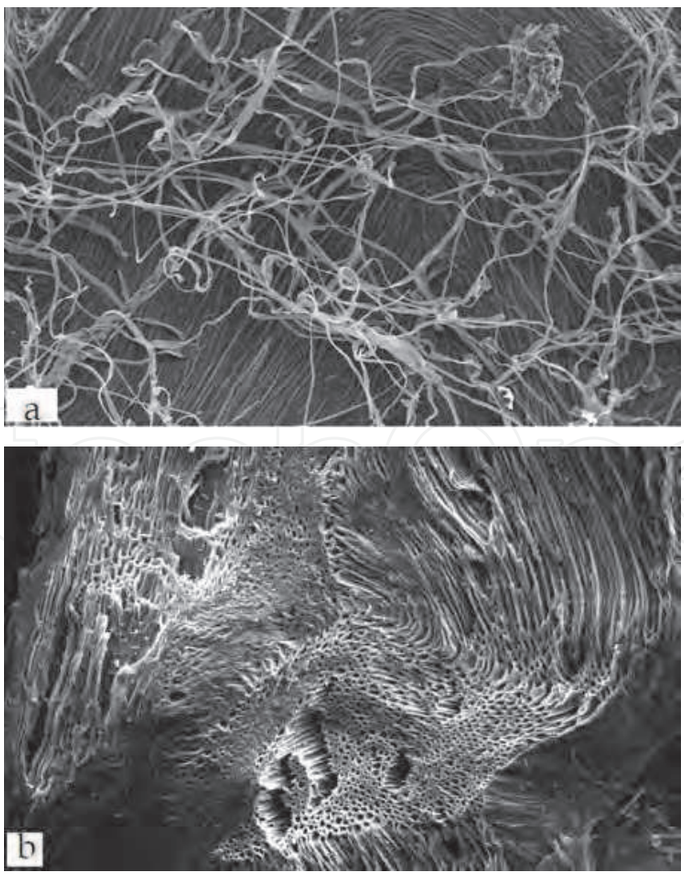

Fig. 3. SEM micrographs of (a) oleaster stones and (b) chars produced from them

3.2 Activated carbon yields

Figure 4 illustrates variations in the yield of activated carbon produced at varying temperatures and conditions. It is evident from the graph that activated carbon yields are affected by the activation method and carbonization temperature. With increasing temperature the yield of activated carbons produced by physical, chemical and sequential activation exhibits a downward trend. The yields obtained through sequential activation were found to be significantly low.

As the process of sequential activation involves the use of both potassium hydroxide and carbondioxide, there is an increase in the decomposition of the structure. In other words, with increasing decomposition more volatiles are released, which leads to a lower yield.

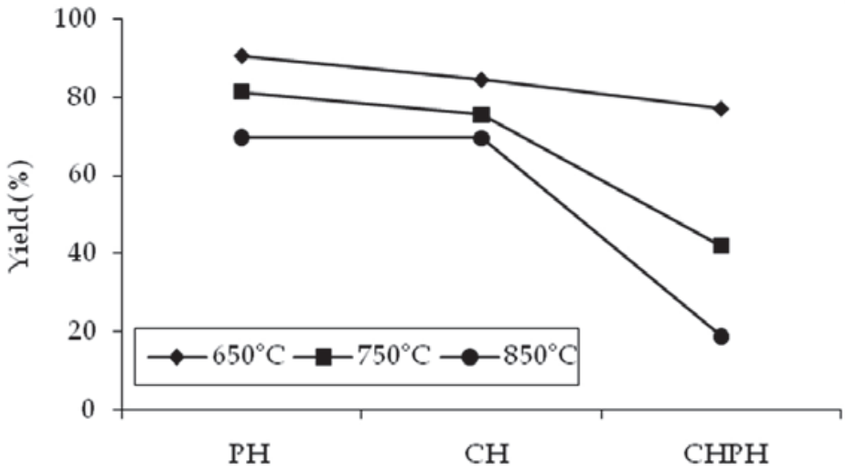

Fig. 4. Variations in activated carbon yields in relation to conditions for the production of activated carbon

3.3 Structural characterization of activated carbons

3.3.1 Isotherms

Figure 5 gives the nitrogen adsorption isotherms at 77K of activated carbons produced at three different temperatures by means of three different methods. An investigation of the adsorption isotherms found them to be isotherms (Type 1) in accordance with IUPAC classification except for activated carbon PH650. Based on this, we can speak of high microporosity (Sing et al., 1985-IUPAC Recommendations).

Adsorption of activated carbons produced at 650ºC, 750ºC and 850ºC displays an upward trend from the lowest to the highest depending on physical, chemical and sequential activation methods in their respective order. Moreover, for each activation method, as temperature increases, so does the adsorption of activated carbons.

The experiments carried out at 650ºC revealed that chemically produced activated carbons have a higher adsorption tendency compared to that of activated carbons produced by physical and sequential methods. There was an increase in the adsorption tendency of activated carbons obtained at 750ºC and 850ºC using all three methods. Activated carbons produced by sequential activation at both temperatures were established to have a comparatively higher adsorption tendency.

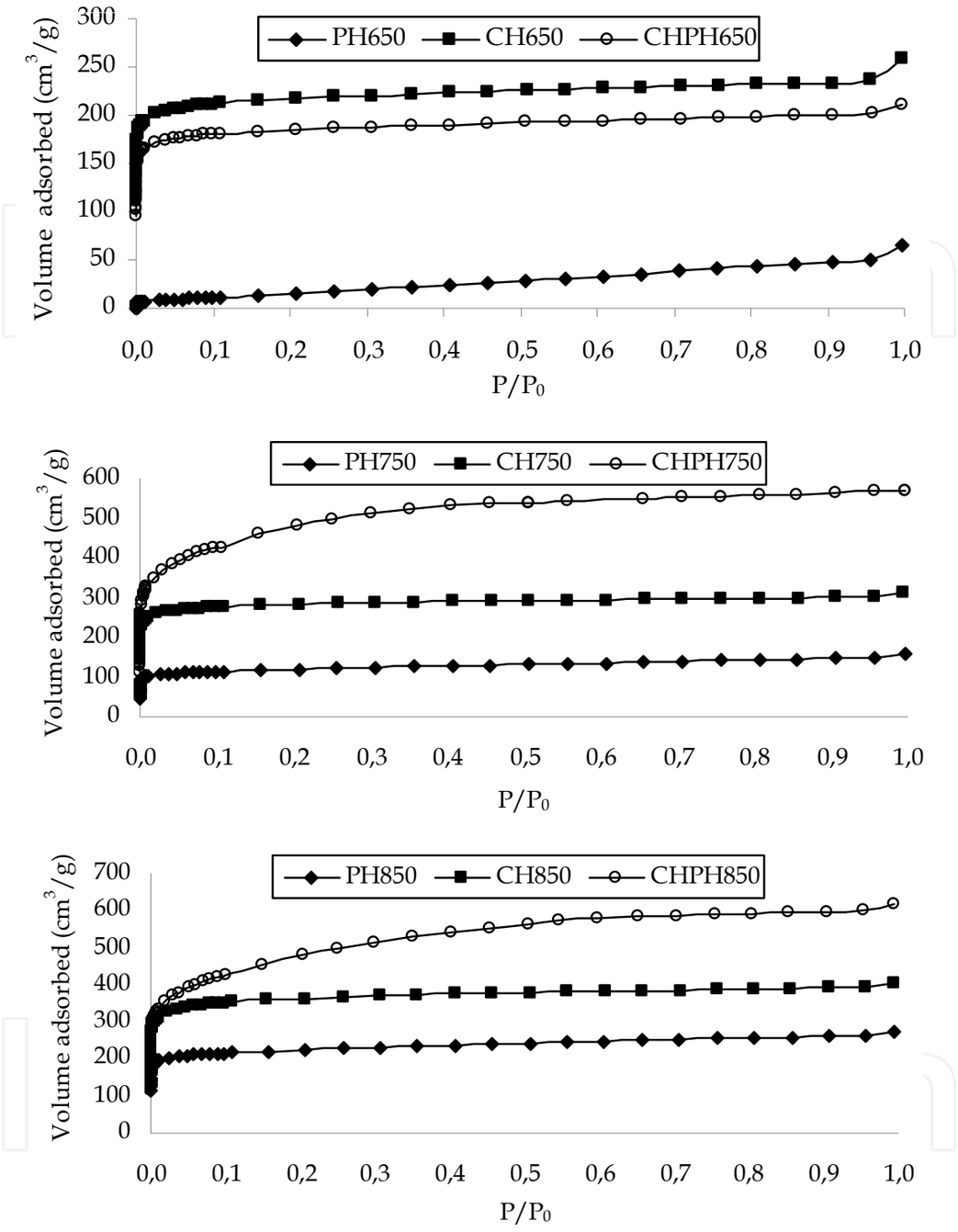

Fig. 5. Nitrogen adsorption isotherms

3.3.2 Surface area

Figure 6 illustrates variations in BET and micropore surface areas of activated carbons produced under three different activation conditions and at three different temperatures. The graph shows that BET and micropore surface areas exhibit variations depending on the activation method and temperature.

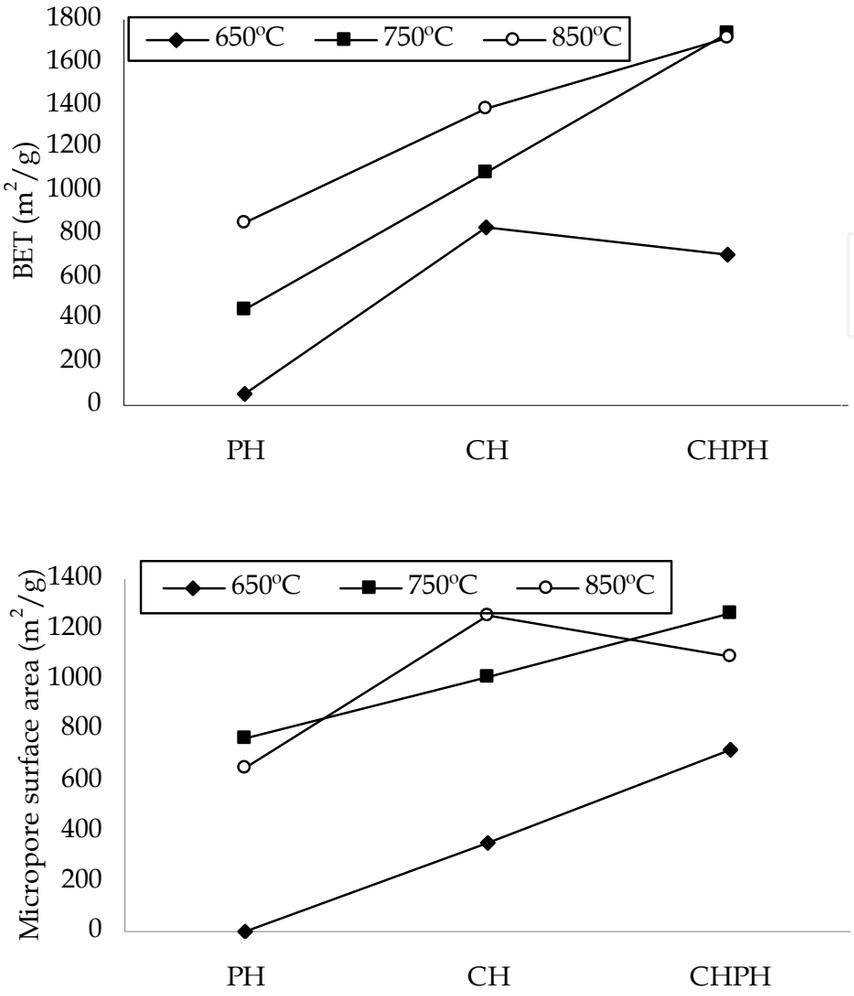

Fig. 6. Variations in BET and micropore surface areas in relation to activation method and temperature

The highest BET and micropore surface area were achieved at a carbonization temperature of 650°C through the production of activated carbons by chemical activation. Activated carbons PH650, CH650 and CHPH650 were found to have BET values of 53 m²/g, 830 m²/g and 707 m²/g, respectively. The micropore surface areas of activated carbons PH650, CH650 and CHPH650 were established to be 0 m²/g, 765 m²/g and 650 m²/g, respectively. The BET surface area for PH650 obtained was found to be low and no pores were observed in the microstructure. It can be stated that physical activation is not effective at this carbonization temperature but chemical activation is suitable. The micropore percentage of activated carbons produced through chemical and sequential activation is 92%.

It was found that activated carbons obtained at 750 °C have a comparatively higher surface area than those produced at 650 °C. The BET values of activated carbons PH750, CH750 and CHPH750 were determined to be 447 m²/g, 1084 m²/g and 1733 m²/g, respectively. The same activated carbons were found to have micropore surface areas of 356 m²/g, 1008 m²/g

and 1254 m^2/g, respectively. The percentage of the micropore surface area for PH750, CH750 and CHPH750 were established to be 79%, 93% and 72%, respectively. It is clear |that the chemical and sequential methods at the same carbonization temperature are suitable for producing activated carbons with a high BET and microporosity. However, it was found that sequential activation is more effective at obtaining a higher BET surface area as compared to chemical activation, which is capable of producing structures with micropores.

As for activated carbons produced at a carbonization temperature of 850 ^oC, their surface areas were found to be higher than those produced at the other two temperatures. Activated carbons produced at this temperature by physical activation, chemical activation and sequential activation were found to have BET values of 849 m^2/g, 1387 m^2/g and 1713 m^2/g, respectively. The micropore surface areas of carbons produced by the same methods were established to be 721 m^2/g, 1261 m^2/g and 1094 m^2/g, respectively. The percentage of micropore surface area of activated carbons produced by means of physical, chemical and sequential activation were determined to be 85%, 91% and 64%, respectively. The BET surface areas were observed to display an upward trend in the order of physical, chemical and sequential activation. In contrast, sequential activation yields a lower micropore surface area. This decrease is attributable to the fact that micropores decompose to become larger.

A comparison of each carbonization temperature reveals that activated carbons produced by chemical activation have higher BET values. BET values of activated carbons obtained through sequential activation are higher compared to those of activated carbons produced by means of both physical and chemical activation.

Figure 7 illustrates how total pore and micropore volumes vary depending on the carbonization temperature and activation method employed.

The highest total pore volume (0,4001 cm^3/g) was achieved through chemical activation employed in experiments carried out at a carbonization temperature of 650 ^oC. At the same carbonization temperature, physical activation and sequential activation yielded total pore volumes of 0,1014 cm^3/g and 0,3273 cm^3/g, respectively. Micropore volume displays variation similar to that observed in total pore volume. It was determined that physical activation does not lead to the formation of micropores. Total pore volume obtained through chemical activation and sequential activation were calculated to be 77% and 79%, respectively. Sequential activation at the same carbonization temperature results in micropore volume increasing.

At 750 ^oC total pore volume was observed to increase during physical, chemical and sequential activation. For these activation methods, total pore volumes were found to be 0,2441 cm^3/g, 0,4820 cm^3/g and 0,9529 cm^3/g, respectively. For the same activation methods, the micropore volume percentages have values of 59%, 84% and 55%, respectively. At this temperature, micropore volume obtained by means of chemical activation was determined to be higher compared to that achieved by means of the other methods.

Total pore volume achieved at 850 ^oC was established to be higher than that obtained at the other carbonization temperatures. Physical, chemical and sequential activation at this temperature yielded total pore volumes of 0,4285 cm^3/g, 0,6294 cm^3/g and 0,9557 cm^3/g, respectively. The micropore volume percentages were calculated to be, in the same order of activation methods employed, 68%, 80% and 49%, respectively. Chemical activation produced a higher micropore volume, whereas micropore volume obtained through sequential activation proved to be comparatively lower.

The densest micropore structure was achieved in activated carbons produced through chemical activation at carbonization temperatures of 750ºC and 850ºC. During chemical activation at three cabonization temperatures, KOH reacts with carbon to form an alkali metal carbonate. This, in turn, decomposes at high temperatures, and the resultant carbon dioxide leads to new pores being formed and the micropores becoming larger (Alcanz-Monge & Illan-Gomez, 2008; Nabais et al., 2008; Tseng et al., 2008). As the sequential activation method involved using both KOH and CO_2, the micropores and new pores become larger. With the physical activation method, carbon dioxide proved to be ineffective at forming new pores.

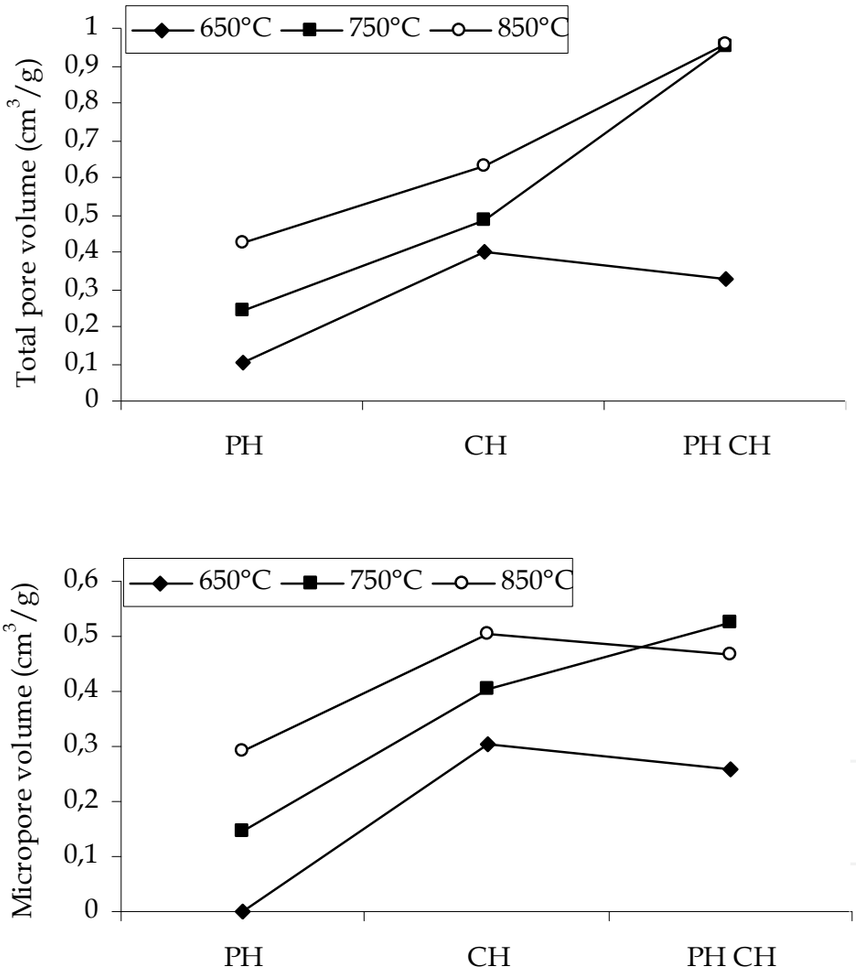

Fig. 7. Variations of total pore and micropore volumes in relation to carbonization temperature and activation method

3.3.3 Pore size distribution

Figure 8 gives variations of pore size distribution calculated based on the DFT method depending on carbonization temperature and the activation method employed.

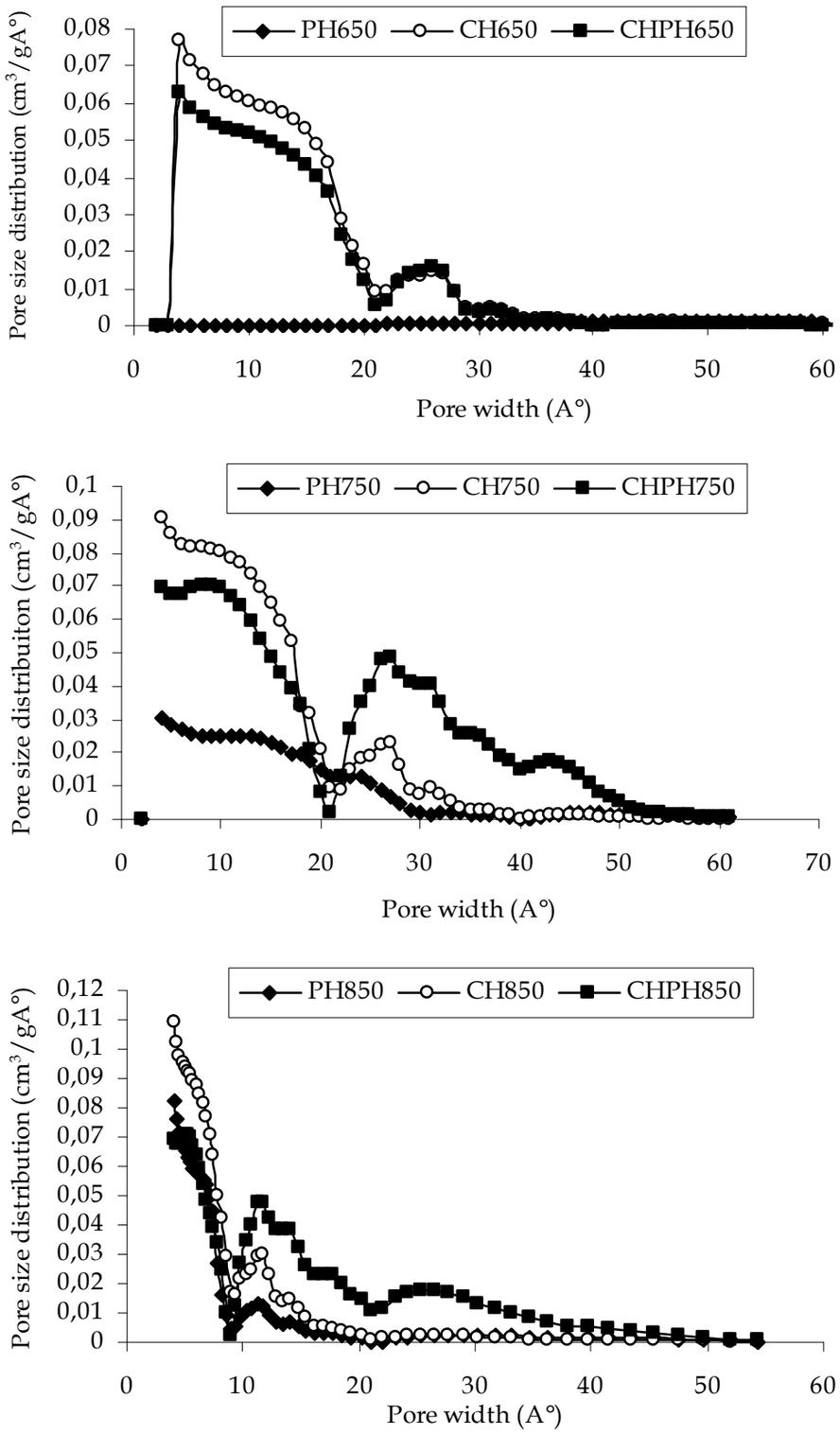

Fig. 8. Variations in pore size distribution in relation to carbonization temperature and activation method

The pore size of activated carbons produced by physical activation at a carbonization temperature of 650 ºC is in the range of 4-55 Aº. Moreover, this activated carbon has a very low BET surface area (53 m²/g) and its micropore surface area could not be determined. The pore size distribution of activated carbons produced through chemical and sequential activation methods is observed to be in the ranges of 2-20 Aº and 20-35 Aº, respectively. This indicates that activated carbons have, along with mesopores, a more dense micropore contents.

A carbonization temperature of 750ºC is observed to lead to both micro- and mesopores forming. Physical activation yielded a pore size distribution in the ranges of 4-20 Aº and 20-30 Aº, chemical activation a pore size distribution in the ranges 4-21 Aº and 21-34 Aº, and sequential activation led to a pore size distribution within the ranges of 4-20 Aº and 20-51 Aº. Chemical activation made it possible for micropores to become more dense at this temperature. As for sequential activation, it was observed to bring about an increase in mesopore density.

It was observed that micropores decrease and mesopores increase even more at a carbonization temperature of 850 ºC. At this temperature, the decomposition of the structure displays an upward trend. Physical activation produced pore size distribution in the ranges of 4-9 Aº and 9-19 Aº, chemical activation led to a pore size distribution ranging from 4 to 9 Aº and from 9 to 19 Aº, and the pore size distribution achieved through sequential activation was within the ranges of 4-9 Aº, 9-12 Aº and 9-19 Aº. At this temperature, new micropores are formed and the existing and new micropores decompose to form mesopores. The densest micropore structure was achieved in activated carbons produced through chemical activation at carbonization temperatures of 750 ºC and 850 ºC.

3.3.4 FTIR spectra

Figure 9 gives FTIR spectra of activated carbons obtained at three different carbonization temperatures using three different activation methods.

The band observed at 3600-3200 cm^{-1} is not present in chars but visible in the spectra of activated carbons produced using the three activation methods. This is because chemical activation and physical activation applied caused oxygen compounds to enter the structure.

The aliphatic groups in the structure of activated carbons are observed at 3000-2800 cm^{-1} . Aromatic structures associated with the band observed 1600-1500 cm^{-1} is not visible in the spectra of activated carbons produced by sequential activation.

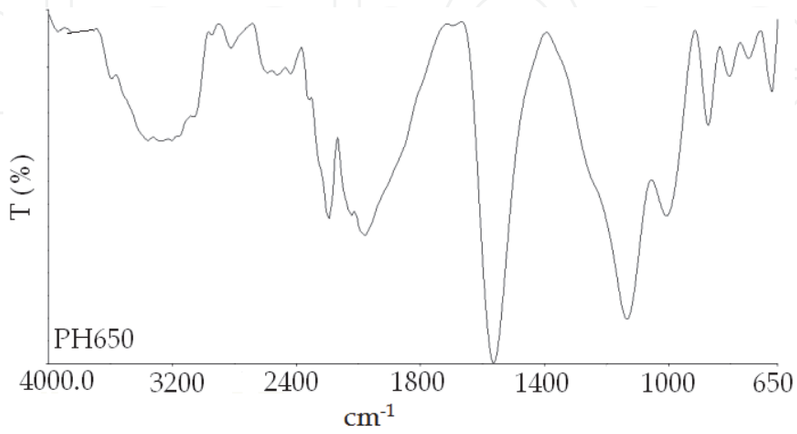

Fig. 9. FITR spectra of activated carbons

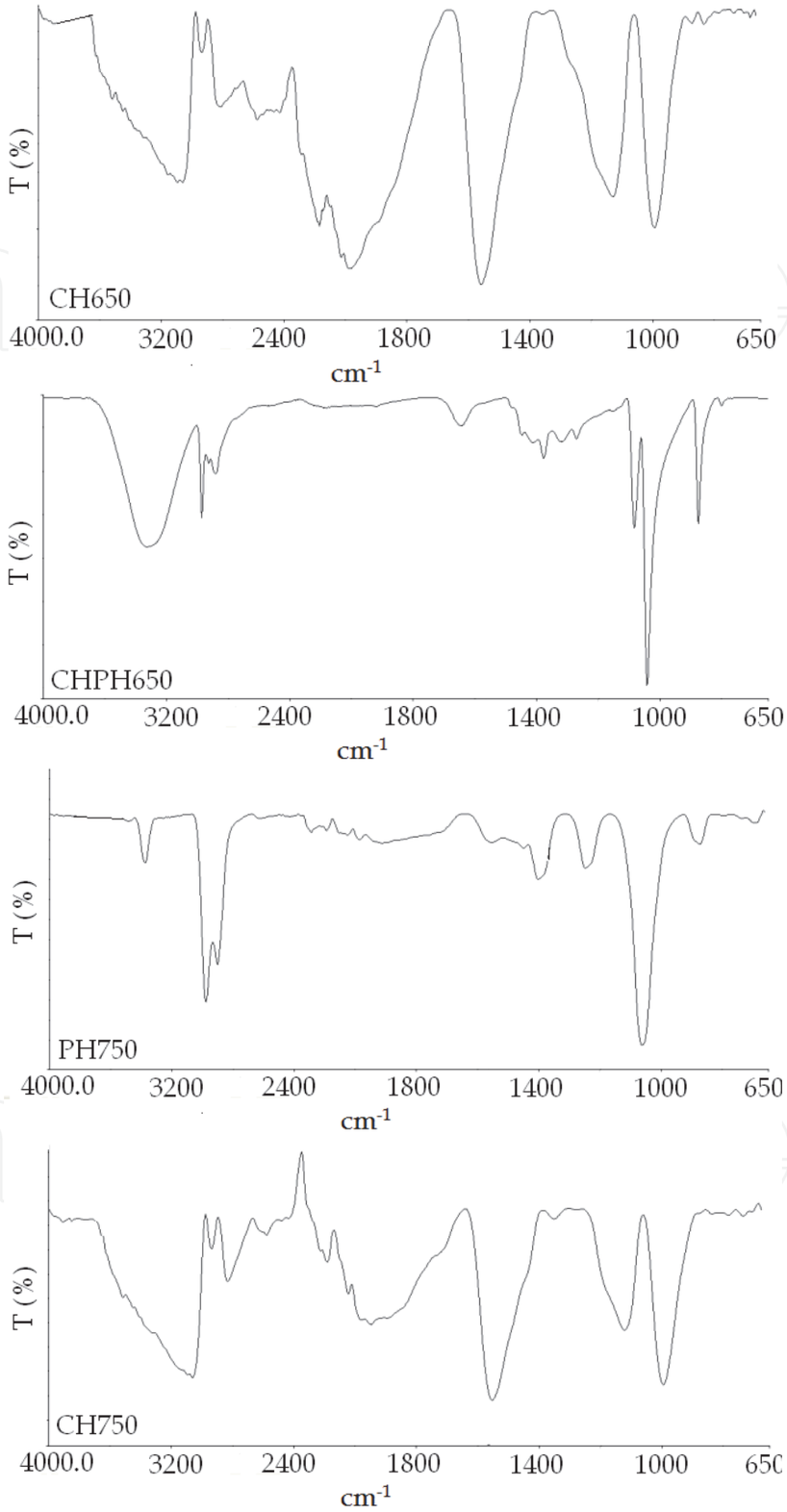

Fig. 9. Continued

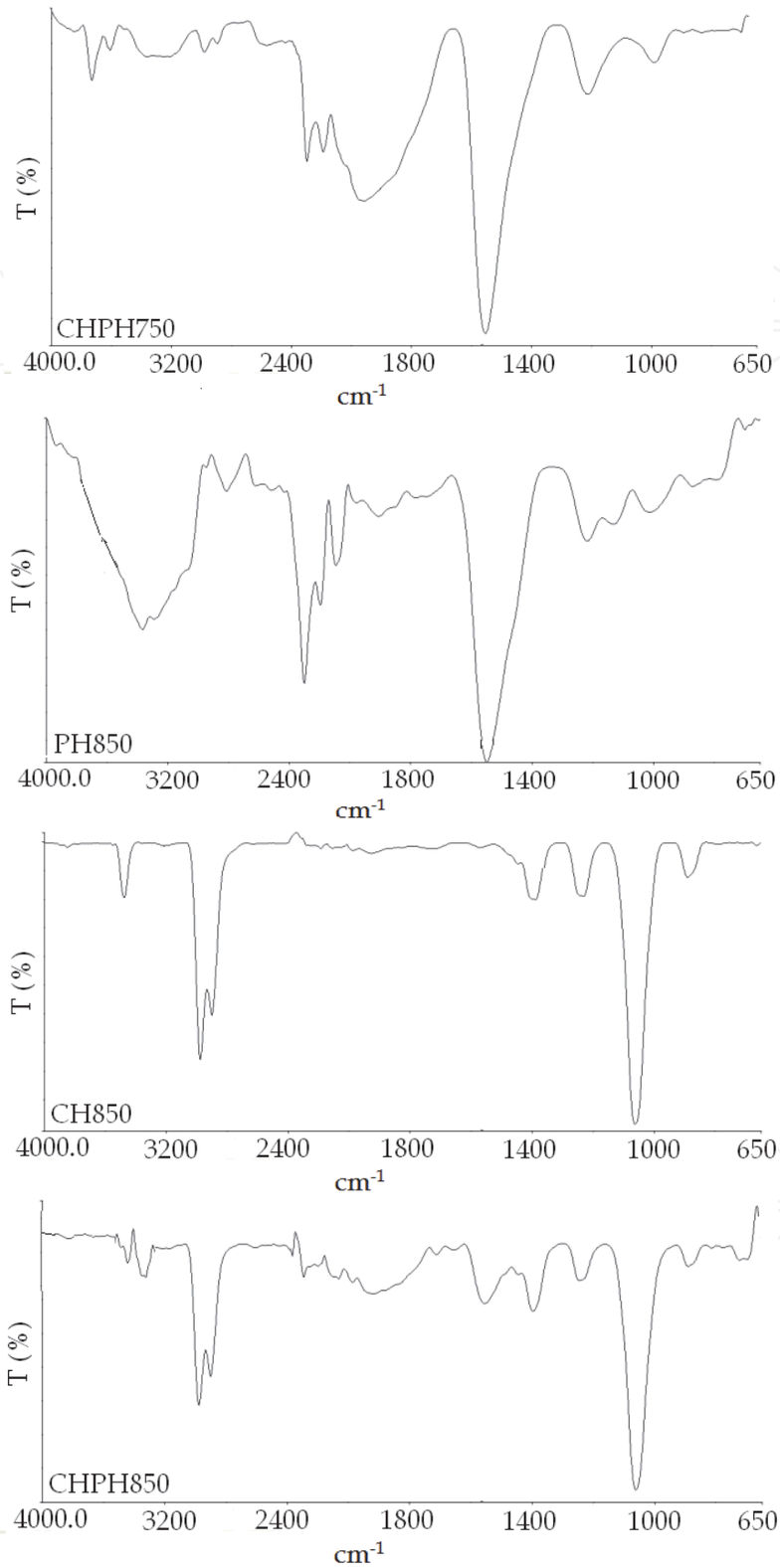

Fig. 9. Continued

Alkene groups at 1450-1300 cm^{-1} are observed as a multiple peak in activated carbons produced using the sequential activation method.
The bands (1240-1000 cm^{-1}) indicative of phenolic and alcoholic structures also occur in activated carbons.
It is evident from the FTIR spectra that functional groups present in oleaster stones decreased, disapeared or became smaller in their chars. Functional groups occurring in the structure of activated carbons produced by physical, chemical and sequential activation at 650°C, 750°C and 850°C exhibited variations as opposed to functional groups in chars. It is evident from the FTIR spectra that the structure of activated carbons was found to contain aromatic, aliphatic and oxygen-containing functional groups.

3.3.5 SEM micrographs

Figure 10 depicts SEM micrographs of activated carbons obtained at three different carbonization temperatures by means of three activation methods.
It can be concluded from SEM micrographs taken during experiments performed at a carbonization temperature of 650°C that the fibers disintegrated and no porous structure was formed. This proves that the value of surface area is low. It is observed that chemical and sequential activation lead to the formation of pores but, do not provide a homogenous distribution.
Physical activation at a carbonization temperature of 750°C was observed to lead to the formation of pores. The chemical and activation methods not only maintained the fibrous structure, but made it possible for pore distribution to be homogenous as well.
Physical activation at a carbonization temperature of 850°C made the porous structure of the activated carbon produced even clearer. In contrast, the chemical and sequential activation methods resulted in the pores decomposing.

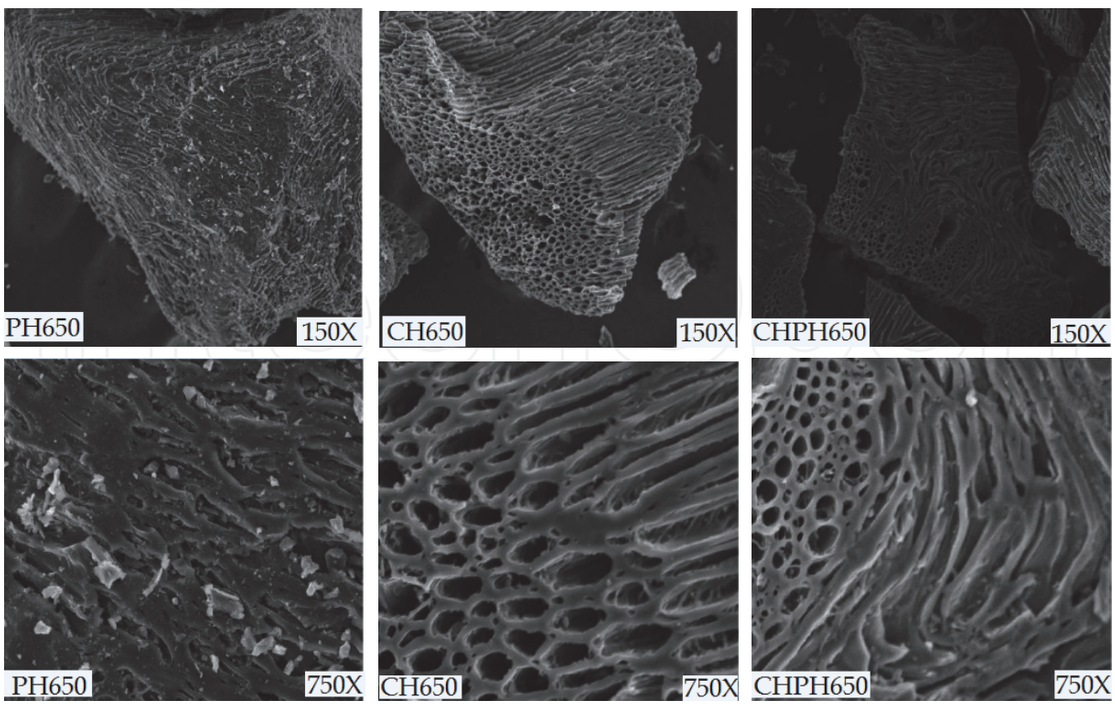

Fig. 10. SEM micrographs of activated carbons (150X and 750X)

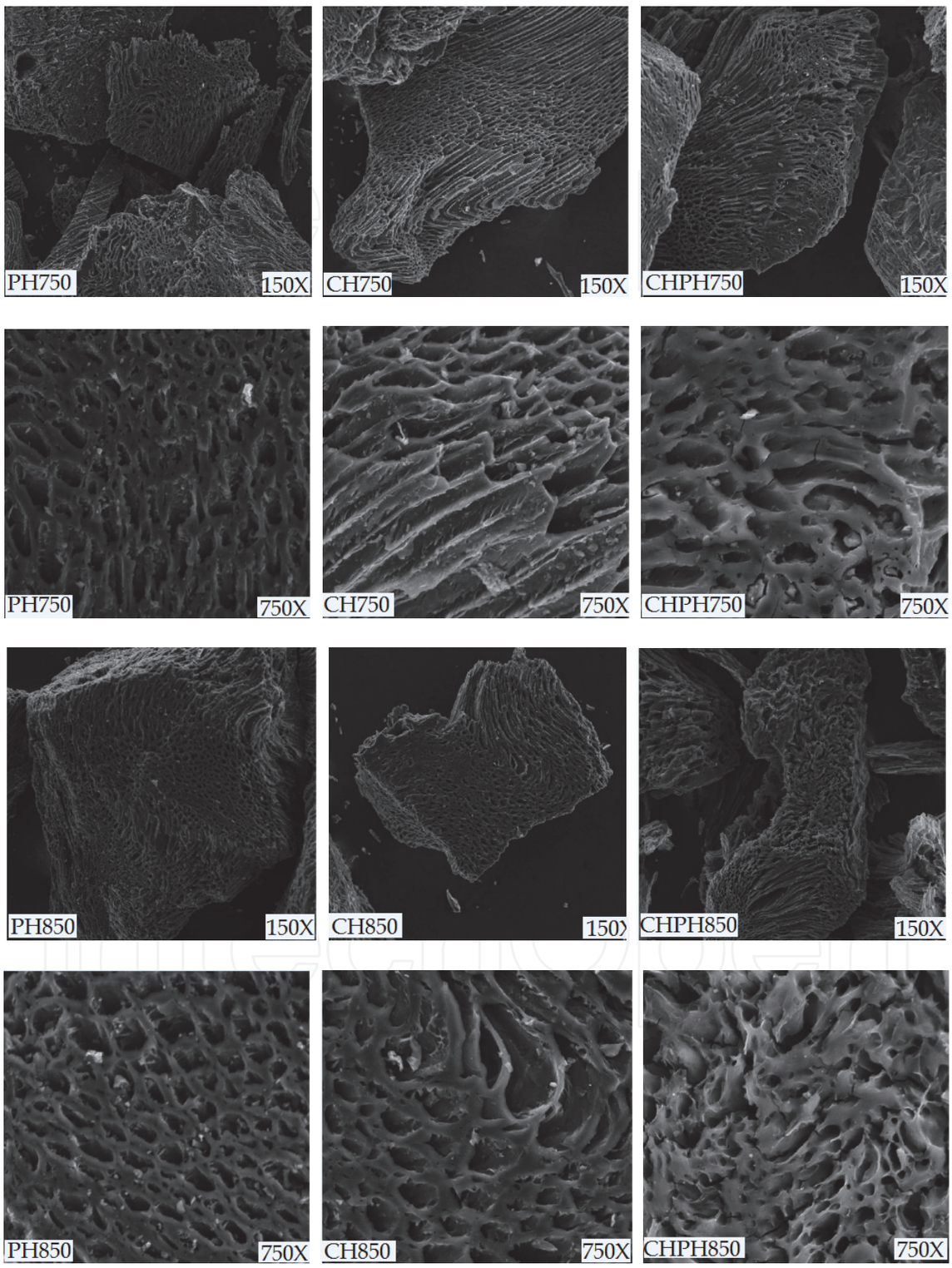

Fig. 10. Continued

3.3.6 Iodine number

The iodine number is a technique employed by producers, sellers, researchers etc. in order to determine the adsorption capacity of activated carbons. The iodine number is the amount of iodine adsorbed by 1g of carbon at the mg level. The iodine value is a measure of porosity for activated carbons. However, no relationship can be established between the iodine number and surface area (ASTM D4607, 2006; Qui&Guo, 2010). The iodine number displays variation depending on the raw material, production conditions and the distribution of the pore volume (ASTM D4607, 2006).

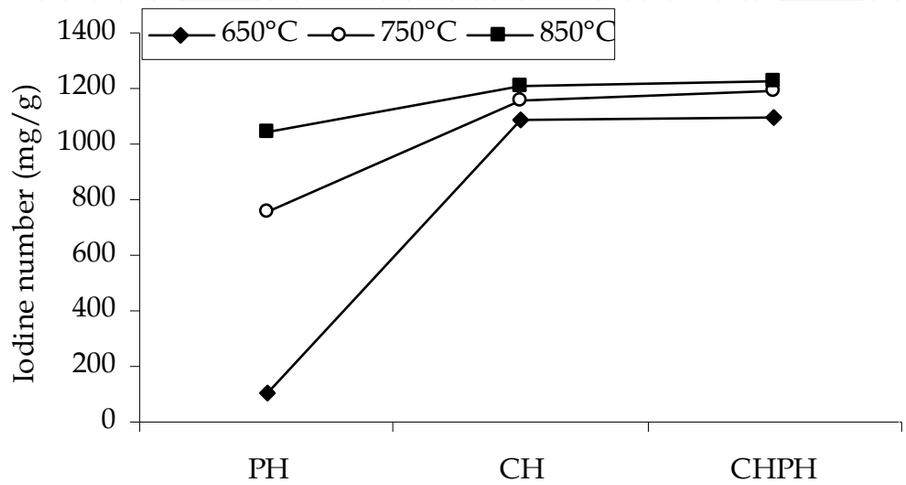

Fig. 11. Variations in the iodine number in relation to the activation method employed and carbonization temperature

Variations in the iodine numbers of activated carbons are given in Table 11. The iodine number is affected by both carbonization temperature and the activation method applied.

4. Conclusion

In this study, I sought to produce activated carbons by physical, chemical and sequential (chemical+physical) activation at carbonizaton temperatures of 650 °C, 750 °C and 850 °C.

It has been established that the porous structure parameters of the activated carbons produced are affected by both carbonization temperature and the activation method employed. The chemical and sequential activation methods led to the formation of activated carbons with a relatively higher BET and micropore surface starting from a carbonization temperature of 750 °C in particular.

Activated carbon produced by means of the sequential activation method at a cabonization temperature of 750 °C yielded the highest BET surface area of 1733 m^2/g. The highest micropore surface area was achieved through chemical activation at a carbonization temperature of 850 °C. By contrast, the highest percentage of micropore surface area with 93% was obtained by means of chemical activation at a carbonization temperature of 750 °C.

The iodine number was also affected by both carbonization temperature and the activation methods employed. Activated carbon obtained at a carbonization temperature of 850 °C using the sequential activation method yielded the highest iodine number.

Also, the FTIR spectra and SEM micrographs taken confirm that, due to their structural characterization, oleaster stones are a suitable material for activated carbon production, and accordingly, use as adsorbents.

5. Acknowledgement

The writer would like to express her gratitude to the Management Zonguldak Karaelmas University Scientific Resaerch Fund (Project No.2008-70-01-01) for their financial assistance at the project level.

6. References

Alcaniz-Monge, J. & Illan-Gomez, M.J. (2008). Insight into hydroxides-activated coals: Chemical or physical activation?, Journal of Colloid Interface Science, Vol. 318, Issue:1, pp. 35-41.

Alcaniz-Monge, J., Perez-Cadenas, M. & Lozano-Castello, D. (2010). Effect of the preoxidation of coals in the preparation of chemically activated carbon pellets, *Energy & Fuels,* Vol. 24, pp. 3385-3393.

Antal, M.J. (1982). Biomass pyrolysis: a review of the literature, Part I carbohydrate pyrolysis, *In Advances in Solar Energy*, (Boer, K.W., Duffie, J.A., Eds.), American Solar Energy Society: Boulder.

ASTM D4607-94 (2006). Standard test method for determination of iodine number of activated carbon.

Aworn, A., Thiravetyan, P. & Nakbanpote, W. (2009) Preparation of CO_2 activated carbon from corncob for monoethylene glycol adsorption, *Colloids And Surfaces A-Physicochemical And Engineering Aspects,* Vol. 333, Issue: 1-3, pp. 19-25.

Aygun, A., Yenisoy-Karakas, S. & Duman, I. (2003). Production of granular activated carbon from fruit stones and nutshells and evaluation of their physical, chemical and adsorption properties, *Microporous and Mesoporous Materials*, Vol. 66, Issue:2-3-, pp. 189-195.

Cuhadaroglu, D. & Uygun, O.A. (2008). Production and characterization of activated carbon from a bituminous coal by chemical activation, *African Journal of Biotechnology*, Vol. 7, Issue: 20, pp. 3703-3710.

Demiral, H., Demiral, I., Tumsek, F. & Karabacakoğlu, B. (2008). Pore structure of activated carbon prepared from hazelnut bagasse by chemical activation, *Surface and Interface Analysis*, Vol. 40, Issue:3-4,pp.616-619.

Demiral, H. & Demiral, I. (2008). Surface properties of activated carbon prepared from wastes, *Surface and Interface Analysis*, Vol. 40, Issue, 3-4, pp.612-615.

Gupta, V.K., Gupta, B., Rastogi, A., Agarwal, S. & Nayak, A. (2011). A comparative investigation on adsorption performances of mesoporous activated carbon prepared from waste rubber tire and activated carbon for a hazardous azo dye-Acid Blue 113, *Journal of Hazardous Materials*, Vol. 186, Issue: 1, pp. 891-901.

Ip, A.W.M., Barford, J.P. & Mckay, G. (2008). Production and comparison of high surface area bamboo derived active carbons, *Bioresource Technology*, Vol. 99, Issue:18, pp. 8909-8916.

IUPAC Manual of symbols and terminology for physicochemical quantities and units. (1972). Butterworths, London.

Jankowska, H. Swiatkowski, A. & Choma, J. (1991). *Active Carbon*, Ellis Horwood.

Kim, D.S. (2004), Activated carbon from peach stones using phosphoric acid activation at medium temperatures, *Journal of Environmental Science and Health Part A-Toxic/Hazardous Substances & Environmental Engineering*, Vol. 39, Issue: 5, pp. 1301-1318.

Kroschwitz, J.I. (Ed.) (1992). *Kirk-Othmer Encyclopeia of Chemical Technology*, John Wiley & Sons.

Liu, L.S., Liu, Z.Y., Yang, J., Huang, Z. & Liu, Z. (2007). Effect of preparation conditions on the properties of a coal-derived activated carbon honeycomb monolith, *Carbon*, Vol. 45, Issue: 14, pp. 2836-2842.

Lu, C., Xu, S. & Liu, C. (2010). The role of K_2CO_3 during the chemical activation of petroleum coke with KOH, *Journal of Analytical and Applied Pyrolysis,* Vol. 87, Issue:2, 282-287.

Luangkiattikhun, P., Tangsathitkulchai, C. & Tangsathitkulchai, M. (2008). Non-isothermal thermogravimetric analysis of oil-palm solid wastes, *Bioresource Technology*, Vol. 99. pp. 986–997.

Marsh, H. & Rodriguez-Reinoso, F. (2006). *Activated Carbon*, Elsevier.

Moreno-Pirajan, J.C., Gomez-Cruz, R., Garcia-Cuello, V.S. & Giraldo, L. (2010). Binary system Cu(II)/Pb(II) adsorption on activated carbon obtained by pyrolysis of cow bone study, *Journal of Analytical and Applied Pyrolysis*, Vol. 89, Issue:1, pp.122-128.

Nabais, J.M., Laginhas, C., Carrott, P.J.M., Ribeiro Carrott, M.M.L., Galacho, C., Amoros, J.E.C. & Gisbert, A.V.N. (2010). Characterization of the surface of activated carbons produced from tire residues, *Materials Science Forum*, Vol. 636-637, pp. 1383-1388.

Nabais, J.V., Carrott, P., Ribeiro Carrott, M.M.L., Luz, V. & Ortiz, A.L. (2008). Influence of preparation conditions in the textural and chemical properties of activated carbons from a novel biomass precursor: The coffee endocarp, *Bioresource Technology*, Vol. 99, No:15, pp.7224-7231.

Ould-Idriss, A., Stitou, M., Cuerda-Correa, E.M., Fernandez-Gonzalez, C., Macias-Garcia, A., Alexandre-Franco, M.F. & Gomez-Serrano, V. (2011). Preparation of activated carbons from olive-tree wood revisited. II. Physical activation with air, *Fuel Processing Technology*, Vol. 92, Issue: 2, pp. 266-270.

Popescu, M.A., Popescu, C.M., Lisa, G. & Sakata, Y. (2011). Evaluation of morphological and chemical aspects of different wood species by spectroscopy and thermal methods, *Journal of Molecular Structure*, Vol. 988, pp. 65–72.

Preethi, S., Sivasamy, A., Sivanesan S, Ramamurthi, V. & Swaminathan, G. (2006). Removal of safranin basic dye from aqueous solutions by adsorption onto corncob activated carbon, *Industrial & Engineering Chemistry Research*, Vol. 45, Issue: 22, pp. 7627-7632.

Sing, K.S.W., Everett, D.H., Haul, R.A.W., Moscou, L., Pierotti, R.A., Rouquerol, J. & Siemieniewska, T. (1985). Reporting physisorption data for gas/solid systems with special reference to the determination of surface area and porosity,, IUPAC Recommendations (1984), *Pure Applied Chemistry*, Vol. 57, No: 4, pp. 603-619.

Singh, Y. (2011). Wealth from waste, Activated Carbon. http://www.wealthywaste.com/activated-carbon

Sun, K. & Jiang, J.C. (2010) Preparation and characterization of activated carbon from rubber-seed shell by physical activation with steam, *Biomass & Bioenergy*, Vol. 34, Issue: 4, pp. 539-544.

Sun, Y., Zhang J.P., Yang, G. & Li, Z.H. (2007). Production of activated carbon by H_3PO_4 activation treatment of corncob and its performance in removing nitrobenzene from water, *Environmental Progress,* Vol. 26, No.1, pp. 78-85.

Soleimani, M. & Kaghazchi, T. (2007) Agricultural waste conversion to activated carbon by chemical activation with phosphoric acid, *Chemical Engineering & Technology*, Vol. 30, Issue: 5, pp. 649-654.

Sutcu, H. & Demiral, H. (2009) Production of granular activated carbons from loquat stones by chemical activation, *Journal of Analytical and Applied Pyrolysis*, Vol. 84, Issue: 1, pp. 47-52.

Sutcu, H. & Dural, A. (2007). The adsorption of lead, copper and nickel ions from aqueous solutions on activated carbon produced from bituminous coal, *Fresenius Environmental Bulletin*, Vol. 16, ıssue: 3, pp. 235-241.

Qiu G. & Guo, M. (2010). Quality of poultry litter-derived granular activated carbon, *Bioresource Technology*, Vol. 101, pp.379-386.

Tongpoothorn, W., Sriuttha, M., Homchan, P. Chanthai, S. & Ruangviriyachai, C. (2011). Preparation of activated carbon derived from Jatropha curcas fruit shell by simple thermo-chemical activation and characterization of their physico-chemical properties, *Chemical Engineering Research and Design*, Vol. 89, pp. 335–340.

Tseng, R.L., Tseng, S.K., Wu, F.C., Hu, C.C. & Wang, C.C. (2008). Effects of micropore development on the physicochemical properties of KOH-activated carbons, *Journal of Chinese Institute of Chemical Engineers,* Vol. 39, Issue: 1, pp.37-47.

Yavuz, R., Akyildiz, H., Karatepe, N. & Çetinkaya, E. (2010). Influence of preparation conditions on porous structures of olive stone activated by H_3PO_4, *Fuel Processing Technology,* Vol. 91, Issue: 1, pp. 80-87.

Yeganeh, M.M., Kaghazchi, T. & Soleimani, M. (2006). Effect of raw materials on properties of activated carbons, *Chemical Engineering & Technology*, Vol. 29, Issue: 10, pp. 1247-1251.

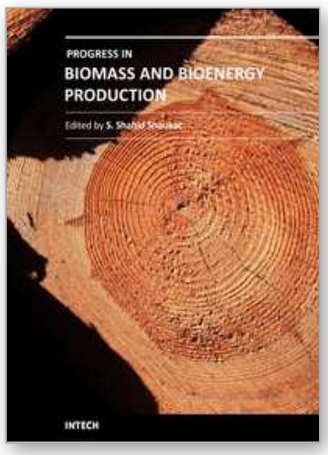

Progress in Biomass and Bioenergy Production
Edited by Dr. Shahid Shaukat

ISBN 978-953-307-491-7
Hard cover, 444 pages
Publisher InTech
Published online 27, July, 2011
Published in print edition July, 2011

Alternative energy sources have become a hot topic in recent years. The supply of fossil fuel, which provides about 95 percent of total energy demand today, will eventually run out in a few decades. By contrast, biomass and biofuel have the potential to become one of the major global primary energy source along with other alternate energy sources in the years to come. A wide variety of biomass conversion options with different performance characteristics exists. The goal of this book is to provide the readers with current state of art about biomass and bioenergy production and some other environmental technologies such as Wastewater treatment, Biosorption and Bio-economics. Organized around providing recent methodology, current state of modelling and techniques of parameter estimation in gasification process are presented at length. As such, this volume can be used by undergraduate and graduate students as a reference book and by the researchers and environmental engineers for reviewing the current state of knowledge on biomass and bioenergy production, biosorption and wastewater treatment.

InTech Europe
University Campus STeP Ri
Slavka Krautzeka 83/A
51000 Rijeka, Croatia
Phone: +385 (51) 770 447
Fax: +385 (51) 686 166
www.intechopen.com

InTech China
Unit 405, Office Block, Hotel Equatorial Shanghai
No.65, Yan An Road (West), Shanghai, 200040, China
中国上海市延安西路65号上海国际贵都大饭店办公楼405单元
Phone: +86-21-62489820
Fax: +86-21-62489821

IntechOpen